

1 **Brain-phenotype predictions can survive across diverse real-world data**

2

3 Brendan D. Adkinson<sup>1</sup>, Matthew Rosenblatt<sup>2</sup>, Javid Dadashkarimi<sup>3,4</sup>, Link Tejavibulya<sup>1</sup>, Rongtao

4 Jiang<sup>5</sup>, Stephanie Noble<sup>5,6,7</sup>, Dustin Scheinost<sup>1,2,5,8,9,10</sup>

5

6 <sup>1</sup> Interdepartmental Neuroscience Program, Yale School of Medicine, New Haven, CT, 06510,

7 USA

8 <sup>2</sup> Department of Biomedical Engineering, Yale University, New Haven, CT, 06520, USA

9 <sup>3</sup> Department of Radiology, Athinoula. Martinos Center for Biomedical Imaging, Massachusetts

10 General Hospital, Charlestown, MA, 02129, USA.

11 <sup>4</sup> Department of Radiology, Harvard Medical School, Boston, MA, 02129, USA.

12 <sup>5</sup> Department of Radiology & Biomedical Imaging, Yale School of Medicine, New Haven, CT,

13 06510, USA

14 <sup>6</sup> Department of Bioengineering, Northeastern University, Boston, MA, 02120, USA

15 <sup>7</sup> Department of Psychology, Northeastern University, Boston, MA, 02115, USA

16 <sup>8</sup> Department of Statistics & Data Science, Yale University, New Haven, CT, 06520, USA

17 <sup>9</sup> Child Study Center, Yale School of Medicine, New Haven, CT, 06510, USA

18 <sup>10</sup> Wu Tsai Institute, Yale University, New Haven, CT, 06510, USA

19

20

21 \*Corresponding author: Brendan Adkinson (brendan.adkinson@yale.edu)

## 22 ABSTRACT

23       Recent work suggests that machine learning models predicting psychiatric  
24    treatment outcomes based on clinical data may fail when applied to unharmonized  
25    samples. Neuroimaging predictive models offer the opportunity to incorporate  
26    neurobiological information, which may be more robust to dataset shifts. Yet, among the  
27    minority of neuroimaging studies that undertake any form of external validation, there is  
28    a notable lack of attention to generalization across dataset-specific idiosyncrasies.  
29    Research settings, by design, remove the between-site variations that real-world and,  
30    eventually, clinical applications demand. Here, we rigorously test the ability of a range of  
31    predictive models to generalize across three diverse, unharmonized samples: the  
32    Philadelphia Neurodevelopmental Cohort (n=1291), the Healthy Brain Network  
33    (n=1110), and the Human Connectome Project in Development (n=428). These  
34    datasets have high inter-dataset heterogeneity, encompassing substantial variations in  
35    age distribution, sex, racial and ethnic minority representation, recruitment geography,  
36    clinical symptom burdens, fMRI tasks, sequences, and behavioral measures. We  
37    demonstrate that reproducible and generalizable brain-behavior associations can be  
38    realized across diverse dataset features with sample sizes in the hundreds. Results  
39    indicate the potential of functional connectivity-based predictive models to be robust  
40    despite substantial inter-dataset variability. Notably, for the HCPD and HBN datasets,  
41    the best predictions were not from training and testing in the same dataset (i.e., cross-  
42    validation) but across datasets. This result suggests that training on diverse data may  
43    improve prediction in specific cases. Overall, this work provides a critical foundation for

44 future work evaluating the generalizability of neuroimaging predictive models in real-

45 world scenarios and clinical settings.

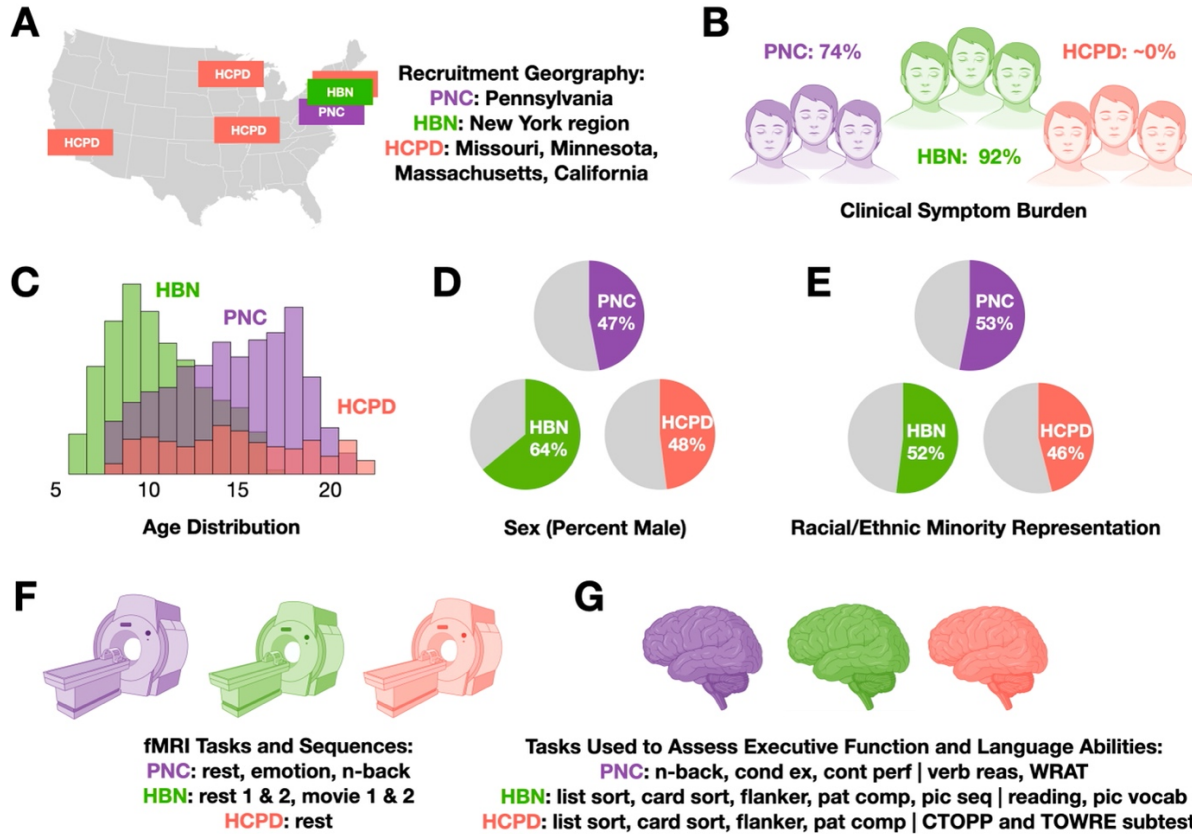
46

## 47 INTRODUCTION

48 Machine learning offers the potential to augment clinical decision-making,  
49 individualize care, and improve patient outcomes (Johnson et al., 2021). Despite this  
50 promise, clinical neurosciences, particularly psychiatry, have yet to realize the advances  
51 in care that have been achieved by other medical disciplines. Recent work highlights  
52 that machine learning models predicting psychiatric treatment outcomes may be  
53 context-dependent and fail when applied to unharmonized samples (*i.e.*, across dataset  
54 shifts) (Chekroud et al., 2024). Given these models rely exclusively on clinical data, the  
55 addition of neurobiologically-grounded data, such as neuroimaging, may help overcome  
56 limitations due to inter-dataset variability (Sui et al., 2020).

57 In light of this, it is imperative to assess whether neuroimaging predictive models  
58 generalize across diverse dataset shifts. Only a minority of neuroimaging studies  
59 undertake any form of external validation. Among those that do, the median external  
60 sample size is only  $n=108$  and is underpowered in most cases (Rosenblatt et al., 2023;  
61 Yeung et al., 2022). Further, real-world and eventual clinical applications demand not  
62 only external validation but also generalization across different imaging and phenotypic  
63 features (Dockès et al., 2021; Woo et al., 2017). By design, many consortium-level  
64 neuroimaging studies remove these variations, creating harmonization that does not  
65 exist in other scenarios. The inclusion of multiple datasets with different imaging  
66 parameters, patient demographics, and behavioral measures is necessary to truly  
67 evaluate a neuroimaging predictive model, as harmonization is not always possible  
68 (Chow et al., 2023; Torres-Espín and Ferguson, 2022). Models will only be clinically  
69 valuable if they can predict effectively on top of these dataset-specific idiosyncrasies.

70 In this work, we rigorously evaluate the external validation of neuroimaging  
71 predictive models across unharmonized samples (Figure 1). We use three distinct,  
72 large-scale developmental datasets: the Philadelphia Neurodevelopmental Cohort  
73 (PNC), the Healthy Brain Network (HBN), and the Human Connectome Project in  
74 Development (HCPD) (Alexander et al., 2017; Satterthwaite et al., 2016; Somerville et  
75 al., 2018). These datasets have high inter-dataset heterogeneity, encompassing  
76 substantial variations in participant characteristics (age distribution, sex, racial and  
77 ethnic minority representation, recruitment geography, clinical symptom burdens),  
78 imaging parameters (fMRI tasks and sequences), and behavioral measures. We used  
79 language abilities and function (EF) as two developmentally and clinically relevant  
80 phenotypes for prediction (Adise et al., 2023; Casey, 2023; Godfrey et al., 2022; Qi et  
81 al., 2021). We demonstrate that reproducible and generalizable brain-behavior  
82 associations using functional connectivity and connectome-based predictive modeling  
83 can be realized across diverse dataset features with sample sizes smaller than  
84 consortium-levels. Results indicate the potential of functional connectivity to be robust  
85 despite various dataset shifts. Further, they provide a critical foundation for future work  
86 evaluating the generalizability of brain-behavior associations in real-world scenarios  
87 and, eventually, clinical settings.



88 **Figure 1. Differences across the PNC, HBN, and HCPD datasets.** The Philadelphia  
89 Neurodevelopmental Cohort (PNC), Healthy Brain Network (HBN), and Human  
90 Connectome Project in Development (HCPD) datasets exhibit a notable lack of  
91 harmonization across recruitment geography (A), participant clinical symptom burden  
92 (B), age distribution (C), sex (D), racial and ethnic minority representation (E), fMRI  
93 tasks and sequences (F), and measures used to assess language abilities and  
94 executive function (G).

95

96

97

98

99

100

101 **RESULTS**

102 We generated models of language abilities and EF in the PNC (n=1291), HBN  
103 (n=1110), and HCPD (n=428) datasets using ridge regression connectome-based  
104 predictive modeling (CPM) (Shen et al., 2017). Connectomes were created using the  
105 Shen 268 atlas. Each participant's connectome included all available resting-state and  
106 task fMRI data with low motion (<0.2 mm). Combining connectomes across fMRI data  
107 improves reliability and predictive power (Elliott et al., 2019; Gao et al., 2019).

108 Participants without one low-motion fMRI run were excluded.

109 A disparate set of behavioral tasks assessed language and EF in the three  
110 datasets (Table S1). We used principal component analysis (PCA) to derive “latent”  
111 factors of language abilities and EF within each dataset. Participants with missing  
112 language and EF measures were excluded. Importantly, the PCA was estimated using  
113 participants who did not have imaging data to maintain proper separation of training and  
114 testing data. The first principal component explained 70%, 55%, and 77% of language  
115 ability measure variance in PNC, HBN, and HCPD, respectively. For executive function,  
116 the first principal component of all behavioral measures explained 53%, 48%, and 40%  
117 of the variance in PNC, HBN, and HCPD, respectively. Contributions of individual  
118 measures to the first principal component are presented in Table S1. Behavioral data  
119 from participants with imaging data were projected onto the first principal component.  
120 This projection was used in all CPM analyses unless otherwise specified.

121 Predictive models were trained and tested within each dataset using 100  
122 iterations of 10-fold cross-validation. Model performance was evaluated with Pearson's  
123 correlation (r), representing the correspondence between predicted and observed

124 behavioral scores, along with the cross-validation coefficient of determination ( $q^2$ ) and  
125 mean square error (MSE). Significance was assessed using permutation testing with  
126 1000 iterations of randomly shuffled behavioral data labels. Cross-dataset predictions  
127 were evaluated with Pearson's correlation.

128

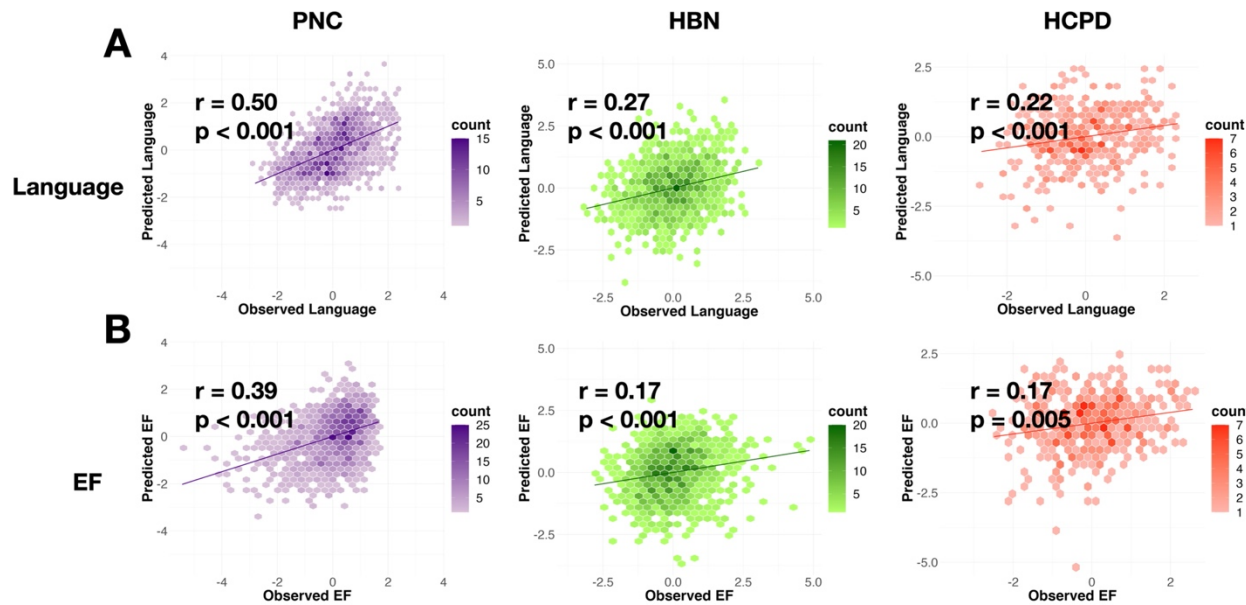
129 **Connectome-based prediction of language abilities**

130 Models successfully predicted language abilities within each dataset (Figures 2A  
131 and S1A; PNC:  $r=0.50$ ,  $p<0.001$ ,  $q2=0.24$ ,  $MSE=1.05$ ; HBN:  $r=0.27$ ,  $p<0.001$ ,  $q2=0.06$ ,  
132  $MSE=4.42$ ; HCPD:  $r=0.22$ ,  $p<0.001$ ,  $q2=0.01$ ,  $MSE=1.47$ ). Model performance was  
133 similar to original predictions when controlling for age, sex, racial/ethnic minority  
134 representation, socioeconomic status, head motion, and clinical symptom burden (Table  
135 S2).

136

137 **Connectome-based prediction of executive function**

138 The performance of EF models closely resembled the performance of language  
139 models (Figures 2B and S1B; PNC:  $r=0.39$ ,  $p<0.001$ ,  $q2=0.14$ ,  $MSE=1.17$ ; HBN:  $r=0.17$ ,  
140  $p<0.001$ ,  $q2=0.02$ ,  $MSE=2.03$ ; HCPD:  $r=0.17$ ,  $p=0.005$ ,  $q2=-0.01$ ,  $MSE=1.98$ ). The  
141 addition of covariates into the model yielded similar results for age, sex, racial/ethnic  
142 minority representation, socioeconomic status, head motion, and clinical symptom  
143 burden (Table S2).



144

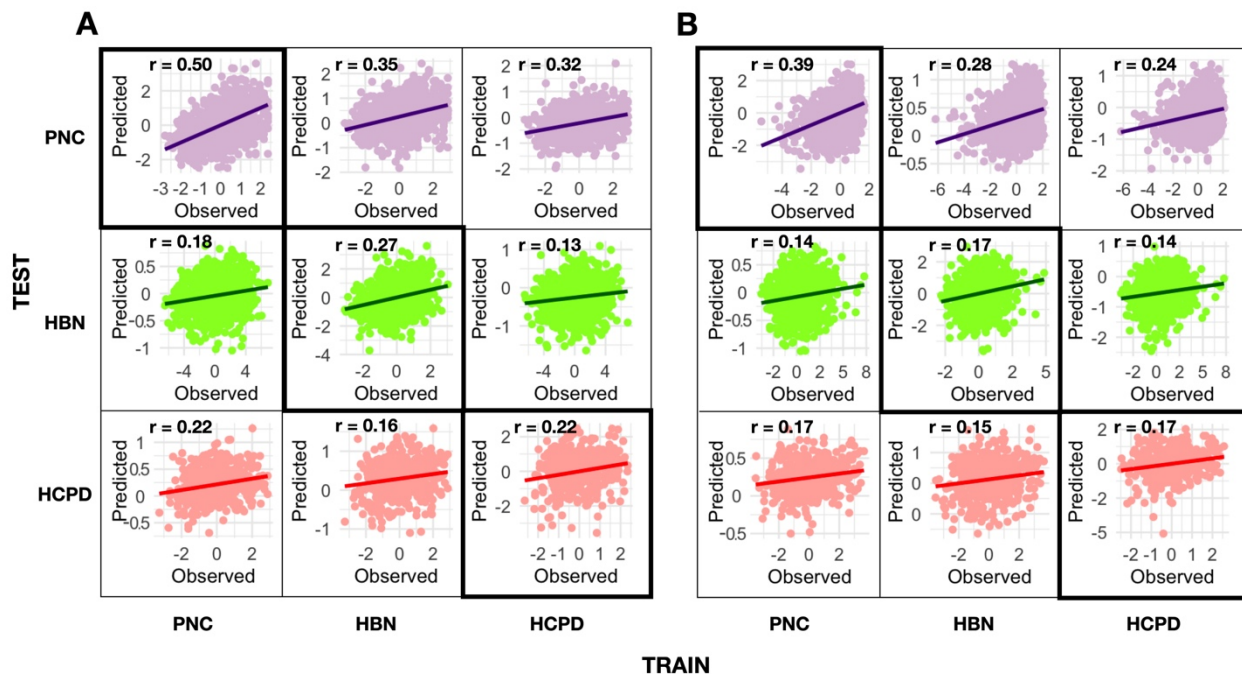
145 **Figure 2. Connectome-based predictive model performance within-dataset.**

146 Scatter plot of observed 1st principal component scores on the x-axis and predicted 1st  
147 principal component scores on the y-axis for language abilities (A) and executive  
148 function (B) across PNC (purple), HBN (green), and HCPD (red). Counts represent  
149 individual participant data.

150

151 **Models generalize across datasets despite notable lack of harmonization**

152 Cross-dataset predictions were performed across the three datasets to ensure  
153 our models' generalizability. Importantly, PNC, HBN, and HCPD are characterized by a  
154 notable lack of inter-dataset harmonization (Figure 1). Despite such substantial  
155 differences, we achieved cross-dataset prediction of language abilities and EF (Figure  
156 3). Language abilities were predicted with  $r$ 's=0.13-0.35. EF was predicted with  
157  $r$ 's=0.14-0.28. Testing on the PNC produced the best cross-dataset predictions for  
158 language abilities and EF. As a result, the best predictions for the HCPD and HBN were  
159 not from training and testing in the same dataset (i.e., cross-validation).



160

161 **Figure 3. Model performances across unharmonized datasets.** Scatter plots of true  
162 versus predicted PCA-derived language abilities (A) and executive function (B) scores  
163 for cross-dataset predictions. Purple (PNC), green (HBN), and red (HCPD) colors  
164 indicate the dataset in which predictions were tested. Diagonals represent within-  
165 dataset prediction performances.

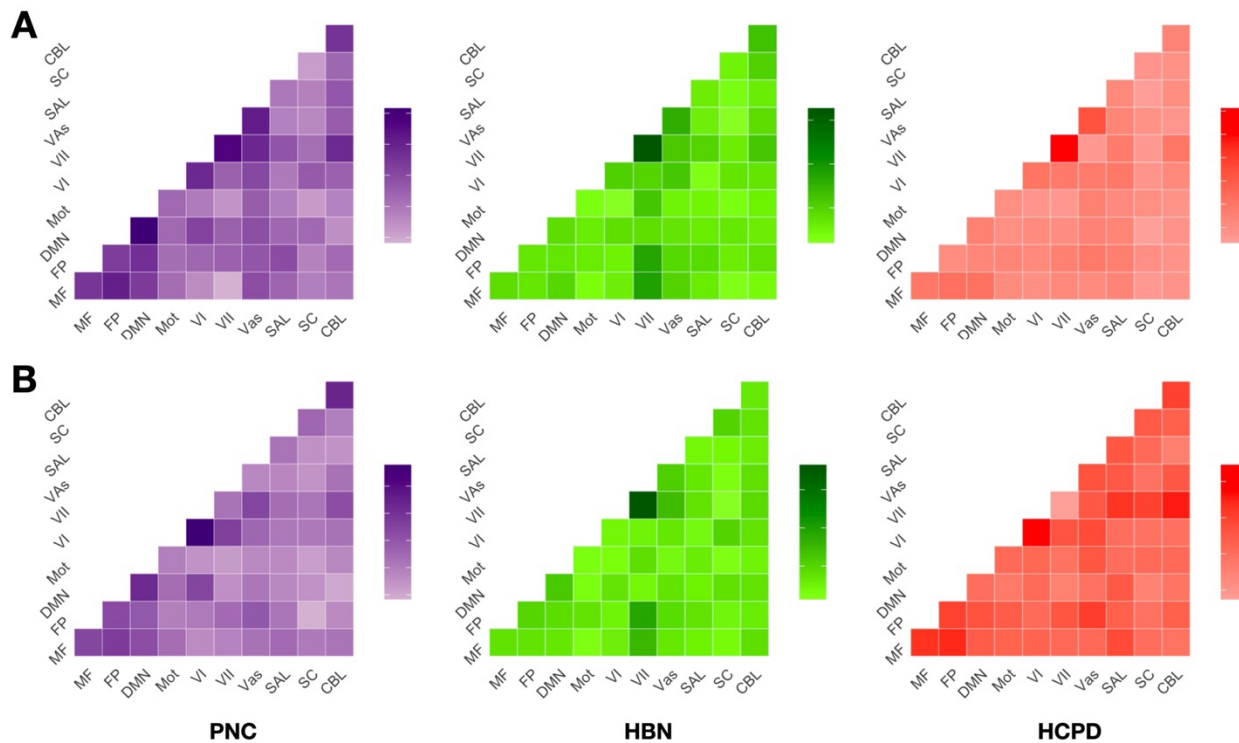
166

### 167 **Brain features underlying language abilities and executive function**

168 In line with previous CPM results, predictive models of language abilities and EF  
169 were complex, with contributions from every node and canonical brain network (Figures  
170 4, S2). Virtual lesioning analyses confirmed the predictive utility of every brain network  
171 but also suggested the importance of the medial frontal and frontoparietal networks in  
172 predicting language abilities and EF (Figure S3). These networks contain noted regions  
173 for language (e.g., Broca's and Wernicke's) and EF (e.g., prefrontal cortex). We  
174 compared the brain features that predicted language abilities and EF in one dataset to

175 those that predicted the same construct in the other two. All edgewise regression  
176 coefficients were normalized by the standard deviation of edges and summed for each  
177 canonical brain network. At the network level, predictive features from each dataset  
178 were correlated between  $r=0.48$ – $0.74$  for language abilities and  $r=-0.03$ – $0.30$  for EF.  
179 The correlations between the HCPD and the HBN or PNC were the lowest (Table S3).  
180

180



181

182 **Figure 4. Network-level contributions to language abilities and executive function**

183 **predictions.** Canonical network contributions to predicted language abilities (A) and

184 executive function (B) across PNC (purple), HBN (green), and HCPD (red).

## 185 Contributions of edges within a single network (diagonals) and between networks (off-

186 diagonals) were defined as the sum of edgewise regression coefficients normalized by

187 network size. Darker colors indicate networks with larger model coefficients. Network

188 Labels: MF, medial frontal; FP, frontoparietal; DMN, default mode; Mot, motor cortex;

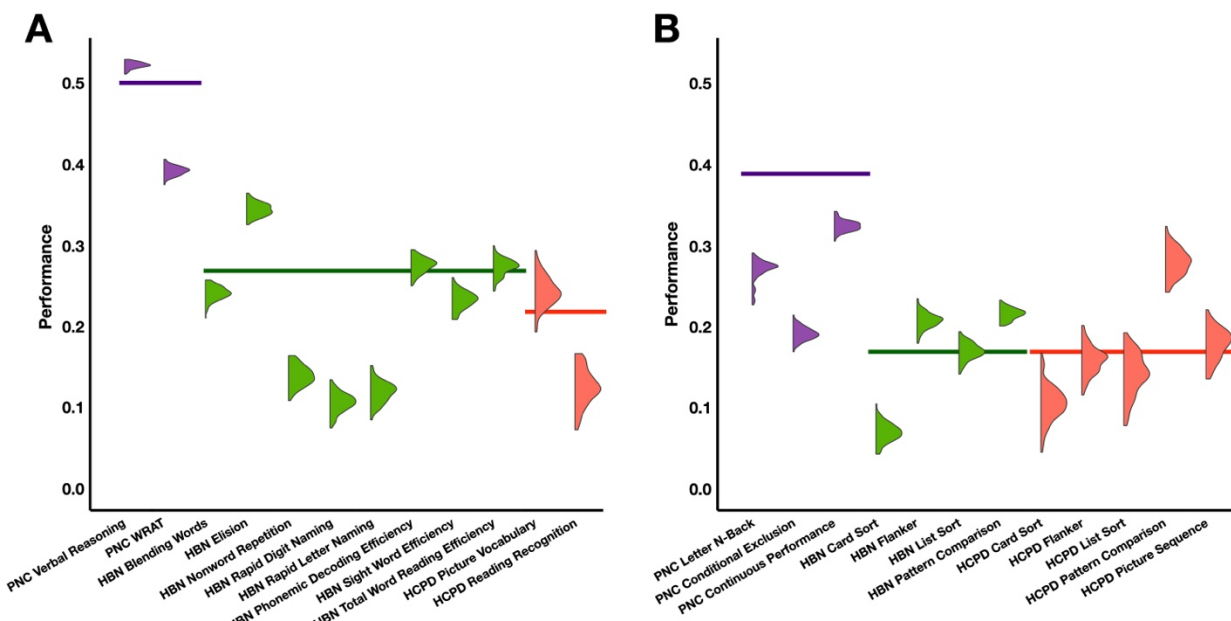
189 VI, visual A; VII, visual B; VAs, visual association; SAL, salience; SC, subcortical; CBL,  
190 cerebellum.

191

## 192 **Prediction of individual language and EF measures**

193 Finally, we tested within and cross-dataset predictions for each measure used in  
194 the PCA. This analysis ensures that the strong cross-dataset predictions are not solely  
195 a function of combining disparate measures. Within-dataset predictions were significant  
196 across all individual measures, with the lowest being the HBN Card Sort task ( $r=0.07$ ,  
197  $p=0.05$ , Figure 5).

198



199  
200 **Figure 5. Within-dataset predictions of individual measures.** Distributions of  
201 prediction performance Pearson's r values across 100 iterations for each individual  
202 language (A) and EF (B) measure. PNC measures are purple, HBN measures are

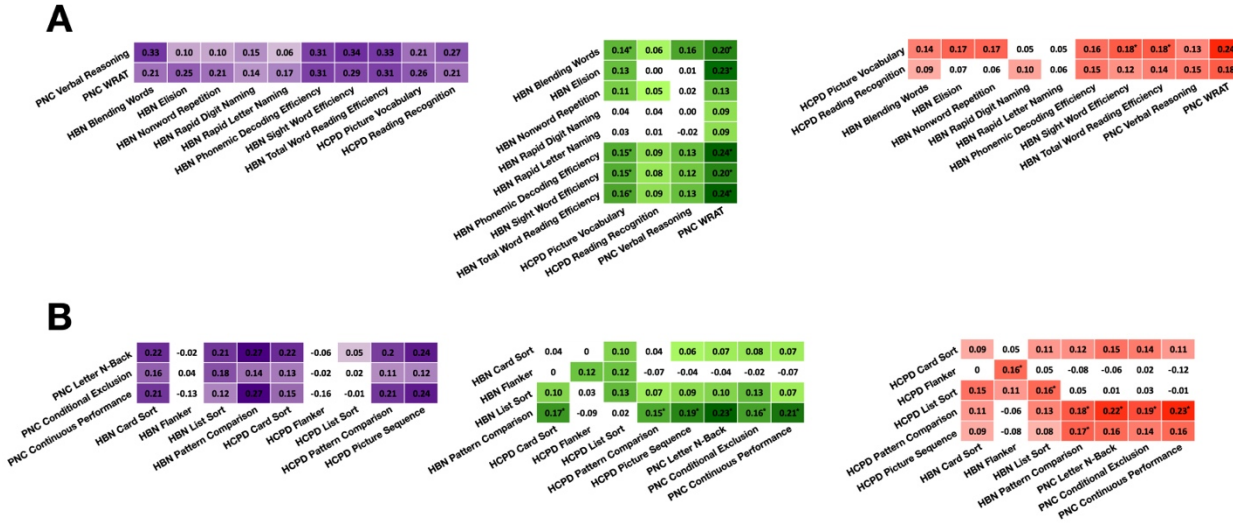
203 green, and HCPD measures are red. Solid lines indicate PCA prediction performances  
204 for comparison.

205

206 Cross-dataset predictions for the individual measures followed patterns similar to  
207 PCA-derived predictions and, in general, were significant (Figure 6). Mirroring PCA  
208 results, cross-dataset language abilities predictions (median  $r=0.14$ , interquartile range  
209 (IQR)=0.09) were more accurate than executive function predictions (median  $r=0.11$ ,  
210 IQR=0.10). For language abilities, all individual measures were predicted in at least one  
211 cross-dataset model. 58 out of 72 cross-dataset models were significant, including all  
212 models tested in the PNC. For EF, 61 out of 94 cross-dataset models were significant.  
213 Models built on the flanker task showed the worst generalization. Most predictions used  
214 different measures in the training and testing data, showing strong generalization of  
215 language and EF models.

216 Finally, we correlated within-dataset and cross-dataset performance. The ability  
217 of a measure to predict measures in another dataset did not correlate with its within-  
218 dataset performance ( $r=0.21$ ,  $p=0.34$ ). However, the ability of a measure to be predicted  
219 by measures in another dataset strongly correlated with within-dataset performance  
220 ( $r=0.72$ ,  $p<0.001$ ). These results indicate that a measure's within-dataset performance  
221 estimates its predictability from other models, but not the predictive ability of its model  
222 on other measures.

223



224

PNC

HBN

HCPD

225 **Figure 6. Cross-dataset predictions of individual measures.** Models were trained on  
226 a single measure in one dataset (x-axis) and independently tested on each individual  
227 measure of the other dataset (y-axis) for language abilities (A) and executive function  
228 (B). Performance r values are shown for PNC (purple), HBN (green), and HCPD (red).  
229 Darker colors indicate higher prediction performances. White indicates non-significant  
230 performances. Asterisks indicate predictions greater than PCA-derived cross-dataset  
231 predictions.

232

233

234

235

236

237

238 **DISCUSSION**

239 We used connectome-based predictive modeling to test the generalizability of  
240 neuroimaging predictive models across diverse dataset features. Predictions of  
241 language abilities and EF survived testing across three unharmonized, large-scale  
242 developmental samples. These results suggest reproducible associations that  
243 overcome individual dataset idiosyncrasies can be achieved with sample sizes (n=500-  
244 1000's) below consortium-level magnitudes. Further, many models based on an  
245 individual measure of language or EF generalized to different language or EF  
246 measures. Interestingly, both PCA and individual measure results indicate that a  
247 model's within-dataset performance estimates its predictability from other models but  
248 not the predictive ability of its model on other measures. Testing brain-behavior  
249 associations across diverse data remains necessary to strengthen the generalizability of  
250 findings beyond a particular dataset and assess applicability to real-world settings.

251 Our results highlight the potential of pooling neuroimaging data without  
252 harmonization. Notably, for the HCPD and HBN datasets, the best predictions were not  
253 from training and testing in the same dataset (i.e., cross-validation) but from external  
254 validation. This result suggests that training on diverse data may improve prediction in  
255 specific cases. Of course, strictly harmonized data collection efforts by consortiums  
256 remain essential (Casey et al., 2018; Sudlow et al., 2015). They maximize statistical  
257 power by minimizing unexplained variance (i.e., experimental noise). Nevertheless,  
258 harmonization is expensive and not always possible (Chow et al., 2023; Torres-Espín  
259 and Ferguson, 2022). It also prevents testing a model's robustness to different  
260 experimental factors. Thus, testing on non-harmonized data is needed. While post-hoc

261 harmonization (i.e., ComBat) is often applied in these studies, we avoided this step to  
262 test how brain-behavior associations can generalize without explicit harmonization  
263 (Chen et al., 2022; Yan et al., 2023). Using non-harmonized sources is a strength of  
264 neuroimaging predictive modeling. Recent work suggests that machine learning models  
265 predicting treatment outcomes from clinical data may fail when applied to unharmonized  
266 samples (Chekroud et al., 2024). Our results point to the potential value of incorporating  
267 neuroimaging data to improve generalization across unharmonized samples.

268 Though our models generalize well, lacking generalization is not inherently bad.  
269 A single model will not be appropriate in all cases. For example, models designed for  
270 adults likely should not work on infants and young children (Scheinost et al., 2023).  
271 Many brain-behavior associations may exhibit sex differences, where sex-specific  
272 models could be needed (Dhamala et al., 2023; Greene et al., 2018; Jiang et al., 2020;  
273 Yip et al., 2023). Further, evidence suggests that those who defy stereotypes (such as  
274 minoritized populations) could require different models (Greene et al., 2022). Rigorously  
275 testing a model on diverse data, regardless of whether it generalizes, produces valuable  
276 information. Null results motivate future studies to understand the lack of generalization  
277 and should be published (Munafò and Neill, 2016). As a field, we should encourage  
278 testing models on diverse data to understand the effects of dataset shift and if models  
279 generalize.

280 We employed state-of-the-field methodology to use as much data as possible.  
281 This approach includes using large sample sizes to create and externally validate  
282 models. In contrast to most studies using external validation, the sample sizes for  
283 external validation were of the same order as the training data (Rosenblatt et al., 2023;

284 Yeung et al., 2022). In fact, given that two external datasets were used to validate each  
285 model, more data was used to test a model than train it. This approach ensured we had  
286 adequate power for external validation. In all cases, we had at least 80% power for  
287 effects as low as  $r=0.15$ . In addition to using large sample sizes, we also used several  
288 fMRI runs and multiple behavior measures for each individual. Combining fMRI and  
289 behavior data improves prediction likely by averaging out the idiosyncrasies of each  
290 data point and increasing reliability. These latent factors also allow diverse data types  
291 (i.e., different fMRI tasks and behavioral measures) to be used for prediction. Finally, we  
292 preserved participants without imaging data to derive principal components (e.g., using  
293 6745 PNC and 1281 HBN participants) to increase the representation. These results  
294 follow the growing appreciation of large (i.e., many participants) and deep (i.e., many  
295 measures per participant) data (Gordon et al., 2017; Marek et al., 2022).

296 Statistical power remains a fundamental consideration in neuroimaging (Cremers  
297 et al., 2017). A rule of thumb is often desired (i.e., 1,000 participants are needed for an  
298 fMRI experiment). However, a simple answer is often insufficient given the complexities  
299 of relating neuroimaging data to behavior. There are too many modalities, behaviors,  
300 and analysis methods. Though, some generalities can be made. Our results  
301 demonstrate that predictive models can generalize across diverse, unharmonized data.  
302 These findings underscore the potential to employ neuroimaging models for predicting  
303 personalized outcomes and finding robust brain-behavior associations (Spisak et al.,  
304 2023). Of course, results will likely be case-specific. Language and EF exhibit large  
305 effect sizes for brain-behavior associations. Other behaviors and phenotypes, such as

306 clinical symptoms, may need larger samples or improved methodology to create robust  
307 associations.

308 Executive function and language abilities are core cognitive processes that are  
309 critical for everyday functioning. Executive function supports manipulating information to  
310 plan, organize, and execute decisions towards goal-directed tasks (Cristofori et al.,  
311 2019; Diamond, 2013). Language abilities support the effective production and  
312 comprehension of communication toward meaningful interaction (Kidd et al., 2018).

313 Cognitive deficits are associated with a range of psychiatric and developmental  
314 disorders (Millan et al., 2012; Zelazo, 2020). Achieving robust predictions of these  
315 constructs is meaningful for cognitive and clinical neuroscience (Barron et al., 2020;  
316 Boyle et al., 2023; Sui et al., 2020). However, the observed effect sizes are still smaller  
317 than necessary for real-world utility. Further, even if our models were actionable, ethical  
318 concerns related to their implementation in developmental populations exist (Scheinost  
319 et al., 2023). For example, false positives lead to unnecessary interventions, while false  
320 negatives divert resources from those who need them. Another consideration is model  
321 interpretability. Clinicians may be more hesitant to trust and integrate less interpretable  
322 models into their practice (Chekroud et al., 2021). The edges we observed contributing  
323 to language abilities and executive function predictions were distributed throughout the  
324 brain. It is difficult to pinpoint a single canonical network responsible for individual  
325 variation in performance (Kohoutová et al., 2020). However, these models align with  
326 recent literature that appreciates complex brain-wide networks rather than the simple  
327 networks often identified by traditional association studies (Dubois et al., 2018).

328        The strength of this study is the rigorous validation of the models. First, we used  
329        three large developmental datasets to maximize statistical power. Few large-scale  
330        neuroimaging studies incorporate any form of external validation (Rosenblatt et al.,  
331        2023; Yeung et al., 2022). In addition to internal cross-validation, each model was  
332        validated in two independent large-scale datasets. Future applications of brain-based  
333        predictive modeling methods must overcome demographics, imaging, and behavioral  
334        data differences. The three datasets exhibited substantial variability in participant  
335        demographics, geographic distribution, and clinical symptoms. Further, the notable lack  
336        of harmonization suggests that these models are not dependent upon specific study  
337        designs or measurement features. Thus, our results are highly generalizable and robust  
338        to dataset shift.

339        Several limitations exist. Using PCA on disparate behavioral measures may  
340        inadvertently remove some elements that make each measure unique. For example,  
341        unique components of EF include working memory, cognitive flexibility, and inhibitory  
342        control. Thus, latent measures from PCA might not represent these components but  
343        instead represent general cognition (Dyer and Kording, 2023). Similarly, we define  
344        language abilities broadly, including receptive language, expressive language, speech,  
345        and reading measures. These broad definitions may also explain the models' lack of  
346        localization. More specific phenotypes will likely improve a model's interpretability  
347        (Enkavi et al., 2019; Greene and Constable, 2023). We also see strong cross-dataset  
348        predictions for individual measures, so testing this hypothesis is plausible for future  
349        work. While our models generalized across various factors, all datasets were

350 developmental samples from the United States. It is unclear if models would generalize  
351 to older individuals or those from non-western countries.

352 In conclusion, we show that brain-behavior associations generated from  
353 functional connectivity data can generalize over non-harmonized data. These results  
354 highlight that generalizable models can be achieved with datasets below consortium-  
355 level sample sizes and the potential of using non-harmonized data. Mimicking real-world  
356 dataset shifts in training and testing predictive models may accelerate their  
357 development into clinical tools and practice.

358

359

360 **METHODS**

361 *Datasets*

362 PNC participants were 1291 individuals ages 8-21 recruited from the greater  
363 Philadelphia, Pennsylvania area (Satterthwaite et al., 2016). Participants completed  
364 rest, emotion task, and n-back task fMRI runs (Satterthwaite et al., 2014). Measures of  
365 language abilities were the Penn Verbal Reasoning Task from the Penn Computerized  
366 Neurocognitive Battery (CNB) and the total standard score from the Wide Range  
367 Assessment Test (WRAT) Reading Subscale (Gur et al., 2010; Wilkinson and  
368 Robertson, 2006). Executive function measures were the Letter N-Back, Conditional  
369 Exclusion, and Continuous Performance tasks from the CNB.

370 HBN participants were 1110 individuals ages 6-17 recruited from the New York  
371 City, New York region (Alexander et al., 2017). Participants completed two rest fMRI  
372 runs as well as 'Despicable Me' and 'The Present' movie-watching scan sessions.  
373 Measures of language abilities were the Elision, Blending Words, Nonword Repetition,  
374 Rapid Digit Naming, and Rapid Letter Naming scaled scores from the Comprehensive  
375 Test of Phonological Processing (CTOPP-2) and the Phonemic Decoding Efficiency,  
376 Sight Word Efficiency, and Total Word Reading Efficiency scaled scores from the Test  
377 of Word Reading Efficiency (TOWRE-2) (Dickens et al., 2015; Tarar et al., 2015).  
378 Executive function measures were the Flanker Inhibitory Control and Attention, List  
379 Sorting Working Memory, Pattern Comparison Processing Speed, and Dimensional  
380 Change Card Sort age-corrected standard scores from the NIH Toolbox (Weintraub et  
381 al., 2013).

382

383 HCPD participants were 428 individuals ages 8-22 recruited from St. Louis,  
384 Missouri, Twin Cities, Minnesota, Boston, Massachusetts, and Los Angeles, California  
385 (Somerville et al., 2018). Participants completed rest fMRI runs (Harms et al., 2018).  
386 Measures of language abilities were the Picture Vocabulary and Oral Reading  
387 Recognition age-corrected standard scores from the NIH Toolbox. Executive function  
388 measures were the Flanker Inhibitory Control and Attention, List Sorting Working  
389 Memory, Pattern Comparison Processing Speed, Dimensional Change Card Sort, and  
390 Picture Sequence Memory age-corrected standard scores from the NIH Toolbox.

391

392 *Preprocessing*

393 In all datasets, data were motion-corrected. Additional preprocessing steps were  
394 performed using BiolImage Suite (Papademetris et al., 2006). This included regression  
395 of covariates of no interest from the functional data, including linear and quadratic drifts,  
396 mean cerebrospinal fluid signal, mean white matter signal, and mean global signal.  
397 Additional motion control was applied by regressing a 24-parameter motion model,  
398 which included six rigid body motion parameters, six temporal derivatives, and the  
399 square of these terms, from the data. Subsequently, we applied temporal smoothing  
400 with a Gaussian filter (approximate cutoff frequency=0.12 Hz) and gray matter masking,  
401 as defined in common space. Then, the Shen 268-node atlas was applied to parcellate  
402 the denoised data into 268 nodes (Shen et al., 2013). Finally, we generated functional  
403 connectivity matrices by correlating each node time series data pair and applying the  
404 Fisher transform. Data were excluded for poor data quality, missing nodes due to lack of

405 full brain coverage, high motion (>0.2mm mean frame-wise motion), or missing  
406 behavioral/phenotypic data.

407

408 *Creating latent factors of language abilities and EF*

409 A principal components analysis (PCA) combined language abilities and EF  
410 measures, respectively, for each dataset. Here, a single behavioral measurement  
411 represents a noisy approximation of the behavioral construct. Combining across  
412 multiple measures reduces this noise. To maintain separate train and test groups in  
413 PNC and HBN, each PCA was limited to participants who did not have usable  
414 neuroimaging data (n=6745 for PNC, n=1281 for HBN).

415

416 *Ridge regression Connectome-based Predictive Modeling*

417 Based on ridge regression, we modify the original CPM framework to better suit  
418 the high-dimensional nature of connectivity data (Gao et al., 2019). Specifically, due to  
419 the positive semi-definite nature of a functional connectivity matrix, the edges are not  
420 independent. Ridge regression is more robust than OLS in this case. Instead of  
421 summing selected edges and fitting a one-dimensional OLS model, we directly fit a  
422 ridge regression model with training individuals using the selected edges from all the  
423 tasks and apply the model to testing individuals in the cross-validation framework. We  
424 trained a ridge regression model using 10-fold cross-validation for the within-dataset  
425 models. We used Pearson's correlation and a feature selection threshold of  $p < 0.05$ .  
426 When controlling for confounds, partial correlation was used for feature selection. The  
427 L2 regularization parameter  $\lambda$  parameter was chosen by an inner 10-fold cross-

428 validation which uses only the training individuals. The largest  $\lambda$  value with a mean  
429 squared error (MSE) within one standard error of the minimum MSE is chosen. This  
430 cross-validation was repeated for 100 random divisions.

431

432 *Model performance*

433 Within dataset prediction was evaluated with a cross-validated coefficient of  
434 determination ( $q^2$ ), and the median  $q^2$  for 100 random 10-fold divisions is reported,  
435 along with Pearson's correlation ( $r$ ) and mean square error (MSE) (Poldrack et al.,  
436 2020). To generate null distributions for significance testing, we randomly shuffled the  
437 correspondence between behavioral variables and connectivity matrices 1,000 times  
438 and re-ran the CPM analysis with the shuffled data. Based on these null distributions,  
439 the p-values for predictions were calculated as in prior work. Only a positive association  
440 between predicted and actual values indicates prediction above chance (with negative  
441 associations indicating a failure to predict), so one-tailed p-values are reported.  
442 Pearson's correlation was tested between actual and predicted values to evaluate  
443 cross-dataset prediction.

444

445 *Model contribution*

446 Predictive networks identified using CPM are complex and composed of multiple  
447 brain regions and networks. To quantify the contribution of each edge to a given  
448 predictive model, we calculated the  $k^{th}$  edge's weight (labeled  $W_{k,}$ ) to the model as:  
449  $W_k = \text{abs}(\beta^{-k}) \text{std}(E_k)$ , where  $\text{std}(E_k)$  represents the standard deviation of the  $k^{th}$   
450 edge, and  $\beta^{-k}$  represents the weight learned by CPM for the  $k^{th}$  edge. To quantify the

451 contribution of each node to a given predictive model, we calculated the  $n^{th}$  node's  
452 weight summed across all edges (labeled  $W_n$ ) to the model as:  $W_n = \sum_{k=1}^{35,778} W_k$ , for all  
453  $k$  edges connected to the  $n^{th}$  node. Next, for the network level,  $W_k$  was averaged over  
454 each edge within or between canonical functional networks.

455

456 *Virtual lesioning*

457 CPM predictive networks are typically widespread and complex, so we  
458 conducted a virtual lesion analysis. For a CPM-based virtual lesion analysis, predictive  
459 networks can be set to zero to examine the degradation in predictive performance  
460 attributed to a virtual lesion of that network (Yip et al., 2020). We iteratively set each  
461 functional network to zero and examined how this impacted the model performance. We  
462 conducted this virtual lesion analysis for the canonical functional networks: medial  
463 frontal (MF), frontoparietal (FP), default mode (DMN), motor (MOT), visual I (VI), visual  
464 II (VII), visual association (VA), salience (SAL), subcortical (SC), and cerebellum (CBL).

465

466 *Data availability*

467 Data are available through the Healthy Brain Network Dataset  
468 (<https://data.healthybrainnetwork.org/main.php>), the Human Connectome Project in  
469 Development Dataset (<https://nda.nih.gov/>), and the Philadelphia Neurodevelopmental  
470 Cohort Dataset ([https://www.ncbi.nlm.nih.gov/projects/gap/cgi-bin/study.cgi?study\\_id=phs000607.v3.p2](https://www.ncbi.nlm.nih.gov/projects/gap/cgi-bin/study.cgi?study_id=phs000607.v3.p2)).

472

473 *Code availability*

474 Preprocessing was carried out using Bioimage Suite, which is freely available:

475 <https://medicine.yale.edu/bioimaging/suite/>. Code for the analyses is available at:

476 <https://github.com/brendan-adkinson/generalization/>.

477

478 *Acknowledgements*

479 Funding: This work was supported by funding from the Wellcome Leap 1kD

480 Program (obtained by D.S.). B.A. was supported by NIH Medical Scientist Training

481 Program Training Grant T32GM136651. M.R. was supported by the National Science

482 Foundation Graduate Research Fellowship under grant DGE2139841. L.T. was

483 supported by the Gruber Science Fellowship. S.N. was supported by the National

484 Institute of Mental Health under grant K00MH122372. Any opinions, findings, and

485 conclusions or recommendations expressed in this material are those of the authors

486 and do not necessarily reflect those of the funding agencies.

487 Competing Interests: B.A. holds equity in Elevation Prep. The authors report no

488 other competing interests.

489

490 **REFERENCES**

491 Adise, S., Ottino-Gonzalez, J., Goedde, L., Marshall, A.T., Kan, E., Rhee, K.E., Goran,  
492 M.I., Sowell, E.R., 2023. Variation in executive function relates to BMI increases  
493 in youth who were initially of a healthy weight in the ABCD Study. *Obesity* 31,  
494 2809–2821. <https://doi.org/10.1002/oby.23811>

495 Alexander, L.M., Escalera, J., Ai, L., Andreotti, C., Febre, K., Mangone, A., Vega-Potler,  
496 N., Langer, N., Alexander, A., Kovacs, M., Litke, S., O'Hagan, B., Andersen, J.,  
497 Bronstein, B., Bui, A., Bushey, M., Butler, H., Castagna, V., Camacho, N., Chan,  
498 E., Citera, D., Clucas, J., Cohen, S., Dufek, S., Eaves, M., Fradera, B., Gardner,  
499 J., Grant-Villegas, N., Green, G., Gregory, C., Hart, E., Harris, S., Horton, M.,  
500 Kahn, D., Kabotyanski, K., Karmel, B., Kelly, S.P., Kleinman, K., Koo, B., Kramer,  
501 E., Lennon, E., Lord, C., Mantello, G., Margolis, A., Merikangas, K.R., Milham, J.,  
502 Minniti, G., Neuhaus, R., Levine, A., Osman, Y., Parra, L.C., Pugh, K.R.,  
503 Racanello, A., Restrepo, A., Saltzman, T., Septimus, B., Tobe, R., Waltz, R.,  
504 Williams, A., Yeo, A., Castellanos, F.X., Klein, A., Paus, T., Leventhal, B.L.,  
505 Craddock, R.C., Koplewicz, H.S., Milham, M.P., 2017. An open resource for  
506 transdiagnostic research in pediatric mental health and learning disorders. *Sci.*  
507 *Data* 4, 170181. <https://doi.org/10.1038/sdata.2017.181>

508 Barron, D.S., Gao, S., Dadashkarimi, J., Greene, A.S., Spann, M.N., Noble, S., Lake,  
509 E.M.R., Krystal, J.H., Constable, R.T., Scheinost, D., 2020. Transdiagnostic,  
510 Connectome-Based Prediction of Memory Constructs Across Psychiatric  
511 Disorders. *Cereb. Cortex N. Y.* 31, 2523–2533.  
512 <https://doi.org/10.1093/cercor/bhaa371>

513 Boyle, R., Connaughton, M., McGlinchey, E., Knight, S.P., De Looze, C., Carey, D.,  
514 Stern, Y., Robertson, I.H., Kenny, R.A., Whelan, R., 2023. Connectome-based  
515 predictive modelling of cognitive reserve using task-based functional connectivity.  
516 *Eur. J. Neurosci.* 57, 490–510. <https://doi.org/10.1111/ejn.15896>

517 Casey, B.J., 2023. Executive functions in the brain, development and social context:  
518 Early contributions by neuroscientist, Adele Diamond. *Dev. Cogn. Neurosci.* 62,  
519 101272. <https://doi.org/10.1016/j.dcn.2023.101272>

520 Casey, B.J., Cannonier, T., Conley, M.I., Cohen, A.O., Barch, D.M., Heitzeg, M.M.,  
521 Soules, M.E., Teslovich, T., Dellarco, D.V., Garavan, H., Orr, C.A., Wager, T.D.,  
522 Banich, M.T., Speer, N.K., Sutherland, M.T., Riedel, M.C., Dick, A.S., Bjork, J.M.,  
523 Thomas, K.M., Chaarani, B., Mejia, M.H., Hagler, D.J., Daniela Cornejo, M.,  
524 Sicat, C.S., Harms, M.P., Dosenbach, N.U.F., Rosenberg, M., Earl, E., Bartsch,  
525 H., Watts, R., Polimeni, J.R., Kuperman, J.M., Fair, D.A., Dale, A.M., ABCD  
526 Imaging Acquisition Workgroup, 2018. The Adolescent Brain Cognitive  
527 Development (ABCD) study: Imaging acquisition across 21 sites. *Dev. Cogn.*  
528 *Neurosci.* 32, 43–54. <https://doi.org/10.1016/j.dcn.2018.03.001>

529 Chekroud, A.M., Bondar, J., Delgadillo, J., Doherty, G., Wasil, A., Fokkema, M., Cohen,  
530 Z., Belgrave, D., DeRubeis, R., Iniesta, R., Dwyer, D., Choi, K., 2021. The  
531 promise of machine learning in predicting treatment outcomes in psychiatry.  
532 *World Psychiatry* 20, 154–170. <https://doi.org/10.1002/wps.20882>

533 Chekroud, A.M., Hawrilenko, M., Loho, H., Bondar, J., Gueorguieva, R., Hasan, A.,  
534 Kambeitz, J., Corlett, P.R., Koutsouleris, N., Krumholz, H.M., Krystal, J.H.,

535                   Paulus, M., 2024. Illusory generalizability of clinical prediction models. *Science*  
536                   383, 164–167. <https://doi.org/10.1126/science.adg8538>

537                   Chen, A.A., Luo, C., Chen, Y., Shinohara, R.T., Shou, H., Alzheimer's Disease  
538                   Neuroimaging Initiative, 2022. Privacy-preserving harmonization via distributed  
539                   ComBat. *NeuroImage* 248, 118822.  
540                   <https://doi.org/10.1016/j.neuroimage.2021.118822>

541                   Chow, S.-M., Nahum-Shani, I., Baker, J.T., Spruijt-Metz, D., Allen, N.B., Auerbach,  
542                   R.P., Dunton, G.F., Friedman, N.P., Intille, S.S., Klasnja, P., Marlin, B., Nock,  
543                   M.K., Rauch, S.L., Pavel, M., Vrieze, S., Wetter, D.W., Kleiman, E.M., Brick,  
544                   T.R., Perry, H., Wolff-Hughes, D.L., Intensive Longitudinal Health Behavior  
545                   Network (ILHBN), 2023. The ILHBN: challenges, opportunities, and solutions  
546                   from harmonizing data under heterogeneous study designs, target populations,  
547                   and measurement protocols. *Transl. Behav. Med.* 13, 7–16.  
548                   <https://doi.org/10.1093/tbm/ibac069>

549                   Cremers, H.R., Wager, T.D., Yarkoni, T., 2017. The relation between statistical power  
550                   and inference in fMRI. *PLoS One* 12, e0184923.  
551                   <https://doi.org/10.1371/journal.pone.0184923>

552                   Cristofori, I., Cohen-Zimerman, S., Grafman, J., 2019. Chapter 11 - Executive functions,  
553                   in: D'Esposito, M., Grafman, J.H. (Eds.), *Handbook of Clinical Neurology, The*  
554                   *Frontal Lobes*. Elsevier, pp. 197–219. <https://doi.org/10.1016/B978-0-12-804281-6.00011-2>

555                   Dhamala, E., Rong Ooi, L.Q., Chen, J., Ricard, J.A., Berkeley, E., Chopra, S., Qu, Y.,  
556                   Zhang, X.-H., Lawhead, C., Yeo, B.T.T., Holmes, A.J., 2023. Brain-Based  
557                   Predictions of Psychiatric Illness-Linked Behaviors Across the Sexes. *Biol.*  
558                   *Psychiatry* 94, 479–491. <https://doi.org/10.1016/j.biopsych.2023.03.025>

559                   Diamond, A., 2013. Executive Functions. *Annu. Rev. Psychol.* 64, 135.  
560                   <https://doi.org/10.1146/annurev-psych-113011-143750>

561                   Dickens, R.H., Meisinger, E.B., Tarar, J.M., 2015. Test Review: Comprehensive Test of  
562                   Phonological Processing–2nd ed. (CTOPP-2) by Wagner, R. K., Torgesen, J. K.,  
563                   Rashotte, C. A., & Pearson, N. A. *Can. J. Sch. Psychol.* 30, 155–162.  
564                   <https://doi.org/10.1177/0829573514563280>

565                   Dockès, J., Varoquaux, G., Poline, J.-B., 2021. Preventing dataset shift from breaking  
566                   machine-learning biomarkers. *GigaScience* 10, giab055.  
567                   <https://doi.org/10.1093/gigascience/giab055>

568                   Dubois, J., Adolphs, R., 2016. Building a Science of Individual Differences from fMRI.  
569                   *Trends Cogn. Sci.* 20, 425–443. <https://doi.org/10.1016/j.tics.2016.03.014>

570                   Dubois, J., Galdi, P., Paul, L.K., Adolphs, R., 2018. A distributed brain network predicts  
571                   general intelligence from resting-state human neuroimaging data. *Philos. Trans. R. Soc. B Biol. Sci.* 373, 20170284. <https://doi.org/10.1098/rstb.2017.0284>

572                   Dyer, E.L., Kording, K., 2023. Why the simplest explanation isn't always the best. *Proc. Natl. Acad. Sci.* 120, e2319169120. <https://doi.org/10.1073/pnas.2319169120>

573                   Elliott, M.L., Knodt, A.R., Cooke, M., Kim, M.J., Melzer, T.R., Keenan, R., Ireland, D.,  
574                   Ramrakha, S., Poulton, R., Caspi, A., Moffitt, T.E., Hariri, A.R., 2019. General  
575                   functional connectivity: Shared features of resting-state and task fMRI drive  
576                   reliable and heritable individual differences in functional brain networks.  
577                   *NeuroImage* 189, 516–532. <https://doi.org/10.1016/j.neuroimage.2019.01.068>

581 Enkavi, A.Z., Eisenberg, I.W., Bissett, P.G., Mazza, G.L., MacKinnon, D.P., Marsch,  
582 L.A., Poldrack, R.A., 2019. Large-scale analysis of test-retest reliabilities of self-  
583 regulation measures. *Proc. Natl. Acad. Sci.* 116, 5472–5477.  
584 <https://doi.org/10.1073/pnas.1818430116>

585 Gao, S., Greene, A.S., Constable, R.T., Scheinost, D., 2019. Combining multiple  
586 connectomes improves predictive modeling of phenotypic measures.  
587 *NeuroImage* 201, 116038. <https://doi.org/10.1016/j.neuroimage.2019.116038>

588 Genon, S., Eickhoff, S.B., Kharabian, S., 2022. Linking interindividual variability in brain  
589 structure to behaviour. *Nat. Rev. Neurosci.* 23, 307–318.  
590 <https://doi.org/10.1038/s41583-022-00584-7>

591 Godfrey, K.J., Espenhahn, S., Stokoe, M., McMorris, C., Murias, K., McCrimmon, A.,  
592 Harris, A.D., Bray, S., 2022. Autism interest intensity in early childhood  
593 associates with executive functioning but not reward sensitivity or anxiety  
594 symptoms. *Autism* 26, 1723–1736. <https://doi.org/10.1177/13623613211064372>

595 Gordon, E.M., Laumann, T.O., Gilmore, A.W., Newbold, D.J., Greene, D.J., Berg, J.J.,  
596 Ortega, M., Hoyt-Drazen, C., Gratton, C., Sun, H., Hampton, J.M., Coalson, R.S.,  
597 Nguyen, A.L., McDermott, K.B., Shimony, J.S., Snyder, A.Z., Schlaggar, B.L.,  
598 Petersen, S.E., Nelson, S.M., Dosenbach, N.U.F., 2017. Precision Functional  
599 Mapping of Individual Human Brains. *Neuron* 95, 791-807.e7.  
600 <https://doi.org/10.1016/j.neuron.2017.07.011>

601 Greene, A.S., Constable, R.T., 2023. Clinical Promise of Brain-Phenotype Modeling: A  
602 Review. *JAMA Psychiatry* 80, 848.  
603 <https://doi.org/10.1001/jamapsychiatry.2023.1419>

604 Greene, A.S., Gao, S., Scheinost, D., Constable, R.T., 2018. Task-induced brain state  
605 manipulation improves prediction of individual traits. *Nat. Commun.* 9, 2807.  
606 <https://doi.org/10.1038/s41467-018-04920-3>

607 Greene, A.S., Shen, X., Noble, S., Horien, C., Hahn, C.A., Arora, J., Tokoglu, F., Spann,  
608 M.N., Carrión, C.I., Barron, D.S., Sanacora, G., Srihari, V.H., Woods, S.W.,  
609 Scheinost, D., Constable, R.T., 2022. Brain-phenotype models fail for individuals  
610 who defy sample stereotypes. *Nature* 609, 109–118.  
611 <https://doi.org/10.1038/s41586-022-05118-w>

612 Gur, R.C., Richard, J., Hughett, P., Calkins, M.E., Macy, L., Bilker, W.B., Brensinger, C.,  
613 Gur, R.E., 2010. A cognitive neuroscience based computerized battery for  
614 efficient measurement of individual differences: Standardization and initial  
615 construct validation. *J. Neurosci. Methods* 187, 254–262.  
616 <https://doi.org/10.1016/j.jneumeth.2009.11.017>

617 Harms, M.P., Somerville, L.H., Ances, B.M., Andersson, J., Barch, D.M., Bastiani, M.,  
618 Bookheimer, S.Y., Brown, T.B., Buckner, R.L., Burgess, G.C., Coalson, T.S.,  
619 Chappell, M.A., Dapretto, M., Douaud, G., Fischl, B., Glasser, M.F., Greve, D.N.,  
620 Hodge, C., Jamison, K.W., Jbabdi, S., Kandala, S., Li, X., Mair, R.W., Mangia, S.,  
621 Marcus, D., Mascali, D., Moeller, S., Nichols, T.E., Robinson, E.C., Salat, D.H.,  
622 Smith, S.M., Sotiropoulos, S.N., Terpstra, M., Thomas, K.M., Tisdall, M.D.,  
623 Ugurbil, K., van der Kouwe, A., Woods, R.P., Zöllei, L., Van Essen, D.C.,  
624 Yacoub, E., 2018. Extending the Human Connectome Project across ages:  
625 Imaging protocols for the Lifespan Development and Aging projects. *NeuroImage*  
626 183, 972–984. <https://doi.org/10.1016/j.neuroimage.2018.09.060>

627 Jiang, R., Calhoun, V.D., Fan, L., Zuo, N., Jung, R., Qi, S., Lin, D., Li, J., Zhuo, C.,  
628 Song, M., Fu, Z., Jiang, T., Sui, J., 2020. Gender Differences in Connectome-  
629 based Predictions of Individualized Intelligence Quotient and Sub-domain  
630 Scores. *Cereb. Cortex N. Y. N* 30, 888–900.  
631 <https://doi.org/10.1093/cercor/bhz134>

632 Jiang, R., Woo, C.-W., Qi, S., Wu, J., Sui, J., 2022. Interpreting Brain Biomarkers:  
633 Challenges and solutions in interpreting machine learning-based predictive  
634 neuroimaging. *IEEE Signal Process. Mag.* 39, 107–118.  
635 <https://doi.org/10.1109/MSP.2022.3155951>

636 Johnson, K.B., Wei, W., Weeraratne, D., Frisse, M.E., Misulis, K., Rhee, K., Zhao, J.,  
637 Snowdon, J.L., 2021. Precision Medicine, AI, and the Future of Personalized  
638 Health Care. *Clin. Transl. Sci.* 14, 86–93. <https://doi.org/10.1111/cts.12884>

639 Kidd, E., Donnelly, S., Christiansen, M.H., 2018. Individual Differences in Language  
640 Acquisition and Processing. *Trends Cogn. Sci.* 22, 154–169.  
641 <https://doi.org/10.1016/j.tics.2017.11.006>

642 Klapwijk, E.T., van den Bos, W., Tamnes, C.K., Raschle, N.M., Mills, K.L., 2020.  
643 Opportunities for increased reproducibility and replicability of developmental  
644 neuroimaging. *Dev. Cogn. Neurosci.* 47, 100902.  
645 <https://doi.org/10.1016/j.dcn.2020.100902>

646 Kohoutová, L., Heo, J., Cha, S., Lee, S., Moon, T., Wager, T.D., Woo, C.-W., 2020.  
647 Toward a unified framework for interpreting machine-learning models in  
648 neuroimaging. *Nat. Protoc.* 15, 1399–1435. <https://doi.org/10.1038/s41596-019-0289-5>

649 Liu, S., Abdellaoui, A., Verweij, K.J.H., van Wingen, G.A., 2023. Replicable brain-  
650 phenotype associations require large-scale neuroimaging data. *Nat. Hum.  
651 Behav.* 7, 1344–1356. <https://doi.org/10.1038/s41562-023-01642-5>

652 Marek, S., Tervo-Clemmens, B., Calabro, F.J., Montez, D.F., Kay, B.P., Hatoum, A.S.,  
653 Donohue, M.R., Foran, W., Miller, R.L., Hendrickson, T.J., Malone, S.M.,  
654 Kandala, S., Feczko, E., Miranda-Dominguez, O., Graham, A.M., Earl, E.A.,  
655 Perrone, A.J., Cordova, M., Doyle, O., Moore, L.A., Conan, G.M., Uriarte, J.,  
656 Snider, K., Lynch, B.J., Wilgenbusch, J.C., Pengo, T., Tam, A., Chen, J.,  
657 Newbold, D.J., Zheng, A., Seider, N.A., Van, A.N., Metoki, A., Chauvin, R.J.,  
658 Laumann, T.O., Greene, D.J., Petersen, S.E., Garavan, H., Thompson, W.K.,  
659 Nichols, T.E., Yeo, B.T.T., Barch, D.M., Luna, B., Fair, D.A., Dosenbach, N.U.F.,  
660 2022. Reproducible brain-wide association studies require thousands of  
661 individuals. *Nature* 603, 654–660. <https://doi.org/10.1038/s41586-022-04492-9>

662 Millan, M.J., Agid, Y., Brüne, M., Bullmore, E.T., Carter, C.S., Clayton, N.S., Connor, R.,  
663 Davis, S., Deakin, B., DeRubeis, R.J., Dubois, B., Geyer, M.A., Goodwin, G.M.,  
664 Gorwood, P., Jay, T.M., Joëls, M., Mansuy, I.M., Meyer-Lindenberg, A., Murphy,  
665 D., Rolls, E., Saletu, B., Spedding, M., Sweeney, J., Whittington, M., Young, L.J.,  
666 2012. Cognitive dysfunction in psychiatric disorders: characteristics, causes and  
667 the quest for improved therapy. *Nat. Rev. Drug Discov.* 11, 141–168.  
668 <https://doi.org/10.1038/nrd3628>

669 Munafò, M., Neill, J., 2016. Null is beautiful: On the importance of publishing null results.  
670 *J. Psychopharmacol. (Oxf.)* 30, 585–585.  
671 <https://doi.org/10.1177/0269881116638813>

673 Noble, S., Scheinost, D., Constable, R.T., 2020. Cluster failure or power failure?  
674 Evaluating sensitivity in cluster-level inference. *NeuroImage* 209, 116468.  
675 <https://doi.org/10.1016/j.neuroimage.2019.116468>

676 Papademetris, X., Jackowski, M.P., Rajeevan, N., DiStasio, M., Okuda, H., Constable,  
677 R.T., Staib, L.H., 2006. BiolImage Suite: An integrated medical image analysis  
678 suite: An update. *Insight J.* 2006, 209.

679 Poldrack, R.A., Huckins, G., Varoquaux, G., 2020. Establishment of Best Practices for  
680 Evidence for Prediction: A Review. *JAMA Psychiatry* 77, 534–540.  
681 <https://doi.org/10.1001/jamapsychiatry.2019.3671>

682 Qi, T., Schaadt, G., Friederici, A.D., 2021. Associated functional network development  
683 and language abilities in children. *NeuroImage* 242, 118452.  
684 <https://doi.org/10.1016/j.neuroimage.2021.118452>

685 Rosenberg, M.D., Finn, E.S., 2022. How to establish robust brain–behavior  
686 relationships without thousands of individuals. *Nat. Neurosci.* 25, 835–837.  
687 <https://doi.org/10.1038/s41593-022-01110-9>

688 Rosenblatt, M., Tejavibulya, L., Camp, C.C., Jiang, R., Westwater, M.L., Noble, S.,  
689 Scheinost, D., 2023. Power and reproducibility in the external validation of brain-  
690 phenotype predictions. *BioRxiv Prepr. Serv. Biol.* 2023.10.25.563971.  
691 <https://doi.org/10.1101/2023.10.25.563971>

692 Satterthwaite, T.D., Connolly, J.J., Ruparel, K., Calkins, M.E., Jackson, C., Elliott, M.A.,  
693 Roalf, D.R., Hopson, R., Prabhakaran, K., Behr, M., Qiu, H., Mentch, F.D.,  
694 Chiavacci, R., Sleiman, P.M.A., Gur, R.C., Hakonarson, H., Gur, R.E., 2016. The  
695 Philadelphia Neurodevelopmental Cohort: A publicly available resource for the  
696 study of normal and abnormal brain development in youth. *NeuroImage* 124,  
697 1115–1119. <https://doi.org/10.1016/j.neuroimage.2015.03.056>

698 Satterthwaite, T.D., Elliott, M.A., Ruparel, K., Loughead, J., Prabhakaran, K., Calkins,  
699 M.E., Hopson, R., Jackson, C., Keefe, J., Riley, M., Mentch, F.D., Sleiman, P.,  
700 Verma, R., Davatzikos, C., Hakonarson, H., Gur, R.C., Gur, R.E., 2014.  
701 Neuroimaging of the Philadelphia neurodevelopmental cohort. *NeuroImage* 86,  
702 544–553. <https://doi.org/10.1016/j.neuroimage.2013.07.064>

703 Scheinost, D., Pollatou, A., Dufford, A.J., Jiang, R., Farruggia, M.C., Rosenblatt, M.,  
704 Peterson, H., Rodriguez, R.X., Dadashkarimi, J., Liang, Q., Dai, W., Foster, M.L.,  
705 Camp, C.C., Tejavibulya, L., Adkinson, B.D., Sun, H., Ye, J., Cheng, Q., Spann,  
706 M.N., Rolison, M., Noble, S., Westwater, M.L., 2023. Machine Learning and  
707 Prediction in Fetal, Infant, and Toddler Neuroimaging: A Review and Primer. *Biol.*  
708 *Psychiatry* 93, 893–904. <https://doi.org/10.1016/j.biopsych.2022.10.014>

709 Shen, X., Finn, E.S., Scheinost, D., Rosenberg, M.D., Chun, M.M., Papademetris, X.,  
710 Constable, R.T., 2017. Using connectome-based predictive modeling to predict  
711 individual behavior from brain connectivity. *Nat. Protoc.* 12, 506–518.  
712 <https://doi.org/10.1038/nprot.2016.178>

713 Shen, X., Tokoglu, F., Papademetris, X., Constable, R.T., 2013. Groupwise whole-brain  
714 parcellation from resting-state fMRI data for network node identification.  
715 *NeuroImage* 82, 403–415. <https://doi.org/10.1016/j.neuroimage.2013.05.081>

716 Somerville, L.H., Bookheimer, S.Y., Buckner, R.L., Burgess, G.C., Curtiss, S.W.,  
717 Dapretto, M., Stine Elam, J., Gaffrey, M.S., Harms, M.P., Hodge, C., Kandala, S.,  
718 Kastman, E.K., Nichols, T.E., Schlaggar, B.L., Smith, S.M., Thomas, K.M.,

719 Yacoub, E., Van Essen, D.C., Barch, D.M., 2018. The Lifespan Human  
720 Connectome Project in Development: A large-scale study of brain connectivity  
721 development in 5–21 year olds. *NeuroImage* 183, 456–468.  
722 <https://doi.org/10.1016/j.neuroimage.2018.08.050>

723 Spisak, T., Bingel, U., Wager, T.D., 2023. Multivariate BWAS can be replicable with  
724 moderate sample sizes. *Nature* 615, E4–E7. <https://doi.org/10.1038/s41586-023-05745-x>

725 Sudlow, C., Gallacher, J., Allen, N., Beral, V., Burton, P., Danesh, J., Downey, P.,  
726 Elliott, P., Green, J., Landray, M., Liu, B., Matthews, P., Ong, G., Pell, J., Silman,  
727 A., Young, A., Sprosen, T., Peakman, T., Collins, R., 2015. UK biobank: an open  
728 access resource for identifying the causes of a wide range of complex diseases  
729 of middle and old age. *PLoS Med.* 12, e1001779.  
730 <https://doi.org/10.1371/journal.pmed.1001779>

731 Sui, J., Jiang, R., Bustillo, J., Calhoun, V., 2020. Neuroimaging-based Individualized  
732 Prediction of Cognition and Behavior for Mental Disorders and Health: Methods  
733 and Promises. *Biol. Psychiatry* 88, 818–828.  
734 <https://doi.org/10.1016/j.biopsych.2020.02.016>

735 Tarar, J.M., Meisinger, E.B., Dickens, R.H., 2015. Test Review: Test of Word Reading  
736 Efficiency—Second Edition (TOWRE-2) by Torgesen, J. K., Wagner, R. K., &  
737 Rashotte, C. A. *Can. J. Sch. Psychol.* 30, 320–326.  
738 <https://doi.org/10.1177/0829573515594334>

739 Torres-Espín, A., Ferguson, A., 2022. Harmonization-Information Trade-Offs for Sharing  
740 Individual Participant Data in Biomedicine. *Harv. Data Sci. Rev.* 4.  
741 <https://doi.org/10.1162/99608f92.a9717b34>

742 Weintraub, S., Dikmen, S.S., Heaton, R.K., Tulsky, D.S., Zelazo, P.D., Bauer, P.J.,  
743 Carlozzi, N.E., Slotkin, J., Blitz, D., Wallner-Allen, K., Fox, N.A., Beaumont, J.L.,  
744 Mungas, D., Nowinski, C.J., Richler, J., Deocampo, J.A., Anderson, J.E., Manly,  
745 J.J., Borosh, B., Havlik, R., Conway, K., Edwards, E., Freund, L., King, J.W.,  
746 Moy, C., Witt, E., Gershon, R.C., 2013. Cognition assessment using the NIH  
747 Toolbox. *Neurology* 80, S54–S64.  
748 <https://doi.org/10.1212/WNL.0b013e3182872ded>

749 Wilkinson, G.S., Robertson, G.J., 2006. Wide Range Achievement Test 4.  
750 <https://doi.org/10.1037/t27160-000>

751 Woo, C.-W., Chang, L.J., Lindquist, M.A., Wager, T.D., 2017. Building better  
752 biomarkers: brain models in translational neuroimaging. *Nat. Neurosci.* 20, 365–  
753 377. <https://doi.org/10.1038/nn.4478>

754 Yan, W., Fu, Z., Jiang, R., Sui, J., Calhoun, V.D., 2023. Maximum Classifier  
755 Discrepancy Generative Adversarial Network for Jointly Harmonizing Scanner  
756 Effects and Improving Reproducibility of Downstream Tasks. *IEEE Trans.*  
757 *Biomed. Eng.* 1–9. <https://doi.org/10.1109/TBME.2023.3330087>

758 Yarkoni, T., 2009. Big Correlations in Little Studies: Inflated fMRI Correlations Reflect  
759 Low Statistical Power—Commentary on Vul et al. (2009). *Perspect. Psychol. Sci.*  
760 4, 294–298. <https://doi.org/10.1111/j.1745-6924.2009.01127.x>

761 Yarkoni, T., Westfall, J., 2017. Choosing prediction over explanation in psychology:  
762 Lessons from machine learning. *Perspect. Psychol. Sci. J. Assoc. Psychol. Sci.*  
763 12, 1100–1122. <https://doi.org/10.1177/1745691617693393>

764

765 Yeung, A.W.K., More, S., Wu, J., Eickhoff, S.B., 2022. Reporting details of  
766 neuroimaging studies on individual traits prediction: A literature survey.  
767 *NeuroImage* 256, 119275. <https://doi.org/10.1016/j.neuroimage.2022.119275>

768 Yip, S.W., Kiluk, B., Scheinost, D., 2020. Toward Addiction Prediction: An Overview of  
769 Cross-Validated Predictive Modeling Findings and Considerations for Future  
770 Neuroimaging Research. *Biol. Psychiatry Cogn. Neurosci. Neuroimaging*,  
771 Understanding the Nature and Treatment of Psychopathology: Letting the Data  
772 Guide the Way 5, 748–758. <https://doi.org/10.1016/j.bpsc.2019.11.001>

773 Yip, S.W., Lichenstein, S.D., Liang, Q., Chaarani, B., Dager, A., Pearlson, G.,  
774 Banaschewski, T., Bokde, A.L.W., Desrivières, S., Flor, H., Grigis, A., Gowland,  
775 P., Heinz, A., Brühl, R., Martinot, J.-L., Martinot, M.-L.P., Artiges, E., Nees, F.,  
776 Orfanos, D.P., Paus, T., Poustka, L., Hohmann, S., Millenet, S., Fröhner, J.H.,  
777 Smolka, M.N., Vaidya, N., Walter, H., Whelan, R., Schumann, G., Garavan, H.,  
778 2023. Brain Networks and Adolescent Alcohol Use. *JAMA Psychiatry* 80, 1131–  
779 1141. <https://doi.org/10.1001/jamapsychiatry.2023.2949>

780 Zelazo, P.D., 2020. Executive Function and Psychopathology: A Neurodevelopmental  
781 Perspective. *Annu. Rev. Clin. Psychol.* 16, 431–454.  
782 <https://doi.org/10.1146/annurev-clinpsy-072319-024242>